Report on research at the Jewish Cemetery in Ostrowiec Świętokrzyski to determine the location of a mass grave from the times of the Holocaust

Authors: Sebastian Różycki, PhD; Szymon Oryński, PhD; Aleksander Schwarz

This report summarises the research carried out by the Zapomniane Foundation and its experts in July, August and October 2024. The research was conducted in accordance with the rules of the Jewish religious law (Halakha) and guidelines of the Rabbinic Commission for Jewish Cemeteries in Poland. The research process consisted of:

- interpretation of historical aerial photos in order to designate the area for further geophysical research in the field,
- geodetic research - marking out the research site and creating a map for non-invasive research,
- geophysical research using GPR (ground-penetrating radar), magnetometer,
- conductometric tests.

Introduction: the characteristic of the research area

Ostrowiec Świętokrzyski is a county town located in central Poland, on the Sandomierz Land in historic Lesser Poland, along the Kamienna River. It is situated in the Świętokrzyskie Voivodeship, which is rich in historical landmarks and tourist attractions. This is a historical place with a rich past that dates back to the Middle Ages. The earliest mentions of the areas that make up the present city date back to the 14th century, and about the village of Ostrów, which gave rise to the city of Ostrowiec, also come from the 14th century. In the interwar period, Ostrowiec developed dynamically thanks to numerous investments related to the construction of the Central Industrial District, which contributed to the economic and urban growth of the city. In 1924, the city significantly expanded its boundaries and was separated from the county self-government association of the Opatów County, which meant greater

autonomy and development opportunities. At the outbreak of World War II, Ostrowiec had about 30,000 inhabitants. In 1929, the city had one church and a synagogue, indicating a diverse religious community. German troops occupied Ostrowiec on September 8, 1939, forcing the population to engage in underground and partisan activities. During World War II and the German occupation, 11,000 Jews from Ostrowiec were brutally murdered. Ostrowiec witnessed numerous public executions, including those whose victims are buried in a sought-after mass grave on the grounds of the former Jewish cemetery.

The geological structure of the surface layers in Ostrowiec Świętokrzyski consists mainly of Holocene and Pleistocene sands and gravel, as well as sands, gravel, peat, river alluvium, and mud in the Kamienna River valley. Locally, on the elevations, there are sands and gravel from the Middle Polish Glaciation (Riss).

Extended interpretation of aerial photographs

Interpretation of archival aerial photographs obtained from the United States National Archives and the Head Office of Geodesy and Cartography for the Ostrowiec Świętokrzyski was carried out by Sebastian Różycki, PhD.

Objective of the study

Our task was to locate a mass grave in the Jewish cemetery in Ostrowiec Świętokrzyski in Poland. The main material used in this task was a photograph taken in October 1945. It showed the Jews of Ostrowiec standing at the site of the mass grave from II WW.

Figure 1. Photos taken in October 1945 in the area of the Jewish cemetery.

Archival Queries

In order to interpret the area of the Jewish cemetery in Ostrowiec Swietokrzyski, archival searches were carried out to find and obtain photogrammetric and cartographic materials. The queries covered the Archives of the United States and the Main Office of Geodesy and Cartography (GUGiK) in Poland.

1939-1945 aerial photographs available in the United States National Archives and Record Administration (NARA), Record Group 373

As part of an order to search for aerial photographs, search queries were performed in the United States National Archives and Records Administration[1] (NARA) for photographs covering the cemetery area in Ostrowiec Świętokrzyski from 1939 to 1945. The search query concerned group 373 collections.

The collections in group 373 comprise sets of aerial and satellite photographs, as well as cartographic and architectural materials. The search query included 373.3 series consisting of aerial photographs taken in 1935 to 1945 by both German and Allied airmen[2].

The photographs available in the archives are shared on a public domain basis. Information from the website of the United States National Archives on public domain, possibility of using and indicating the source:

"The vast majority of the digital images in the Online Catalog are in the public domain. Therefore, no written permission is required to use them. We would appreciate your crediting the National Archives and Records Administration as the original source."

Based on the results of the search query conducted in the archives, a list of photographs was created for the cemetery and the photographs available were ordered in the archives.

The following aerial photos were acquired form NARA: - May 31, 1944 (Luftwaffe − **signature DT TM 3**), - January 19, 1945 (Luftwaffe − **signature GX 12366**), - February 3, 1945 (Luftwaffe − **signature GX 8066**), - April 19, 1964 (Polish Geodetic Survey).

---

[1] The Archives Address: National Archives at College Park, 8601 Adelphi Road, College Park, MD 20740-6001

[2] The collection of photographs taken by the Allied airmen consists of 2,863,800 pieces, and by the German airmen — 1,209,520
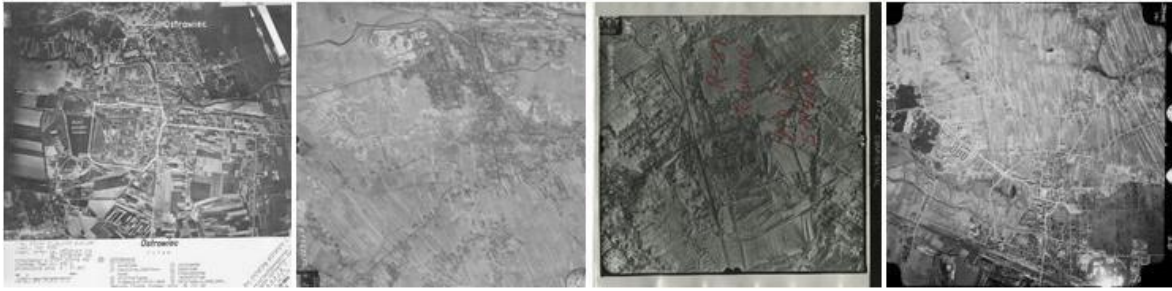
Figure 2. From the left aerial photos from: 05.1944, 01.1944, 02.1945, 04.1964.

Research methodology

To define the boundaries of the mass grave and for the sake of interpretation, archival and current data relating to the surrounding area will be used. Archival data in the form of aerial photographs taken during the second World War and topographical maps are the main material for recreating the boundaries of the cemetery and for analysing the historical coverage of the area.

In some cases, laser scanning data showing the terrain may be a very useful source of information. Current data in the form of aerial photographs will be used to reference (georeference) archival data and will allow visualisation of the selected archival objects on the current background.

QGIS software was used for practical interpretation and analysis of the terrain. In the first stage of the works, vector layers were acquired, showing the cemetery border and the terrain objects and damage seen in the 1944 and 1945 photographs: roads, building remains, and terrain damage. The vector layers created allowed the creation of graphic attachments. All the data obtained from the interpretation have been written to the National Spatial Reference System: system 2000, zone 7. This helped generate geodetic coordinates of the selected objects. These coordinates will allow to map the identified objects in the area in the aerial photographs taken in 1944 and 1945.

Interpretation of an aerial photograph taken in 1944

The entire cemetery was recorded in the photograph from 1944, 1945, 1964 and its interpretation is possible. Their quality is good.

Black and white aerial photographs show the recorded area of the terrain in shades of grey between extreme tones of white and black. The grey tones in the photograms are so-called direct distinguishing features which help identify objects. The tone of the object is closely related to the rays reflected from the object and recorded on the film. The object perpendicular to the light source will reflect the most rays and will be the brightest in the photograph, regardless of the colour it physically has. The tone of the object in the image is also affected by the nature of the surface itself. The smoother the surface, the brighter the tone in the picture. In contrast, the tones in the photograph defining vegetation are dependent on a phenological factor, e.g. green grass is photographed in a dark grey tone and dried grass — in a light tone.

Other direct distinguishing features include the shape, size, and shadow of individual objects.

The shape in aerial photographs is most often used to distinguish natural objects from man-made objects. The latter are characterised by a regular geometric shape. The exterior appearance of a building, in some cases, even allows it sometimes to recognize its purpose (to distinguish between residential and industrial buildings). Shadows are divided into cast shadows and self shadows. When reading, orient the picture with respect to the light source. A cast shadow is a shadow cast by objects on the surface of the ground or on other objects. A self shadow is the shaded part of the photographed object. Based on shadows, you can calculate the height of an item. Remember that the shadow cast onto the dips increases, while it decreases in case of rising terrain. Also note that when the sun is low above the horizon (e.g. in the morning), the shadows will be longer, causing the object to deform.

The process of interpretation of aerial photographs

In photos taken in 1945, buildings are visible in the background. To locate the mass grave in the first place, the layout of streets and buildings that no longer exist was reconstructed. In order to reproduce the largest part of the city, 2 photos were merged together (using the image matching technique – fig. 3).

Figure 3. Numbers indicate the buildings visible in 1945 and the road.

The visible buildings (numbers 1-3) and the road (number 4) were reconstructed on the basis of a 1945 aerial photo (fig. 4).
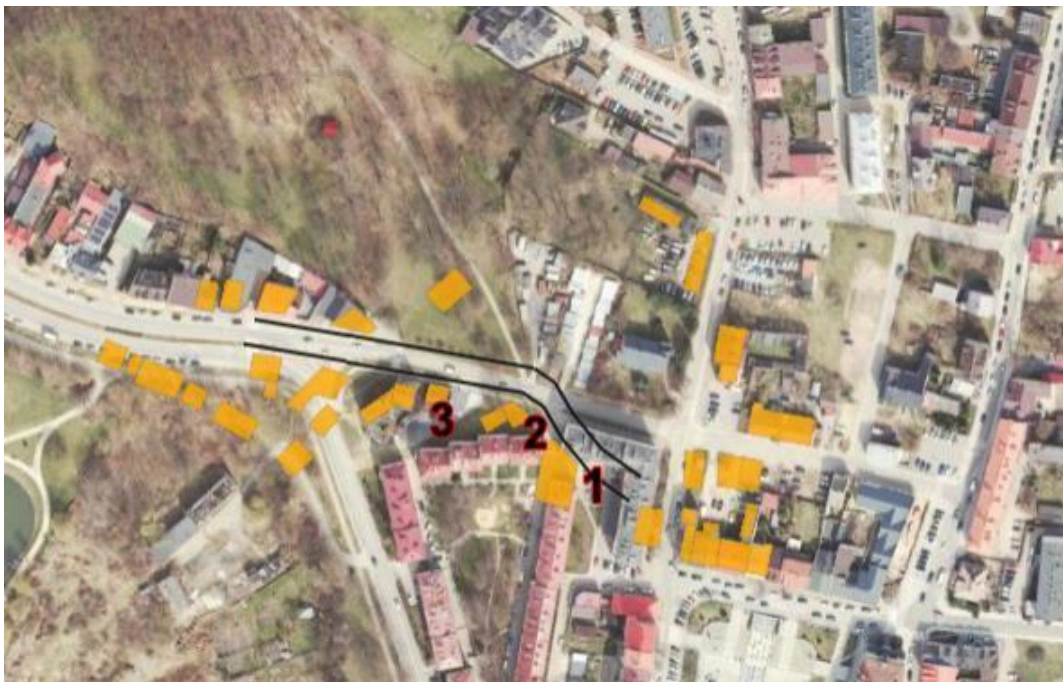

Figure 4: buildings from 1945. Visible outline and course of the 1945 road (black lines). An orthophoto from 2022 was used as a base.

The paths that were in the cemetery were also reconstructed based on 1945 aerial photos. The 1945 photos show snow, so the trampled paths are clearly visible.

Figure 5 : buildings from 1945. Visible outline and course of the 1945 road (black lines). The pins have been marked with photos of buildings that are in the background of the main photo.
An orthophoto from 1945 was used as a base.

To locate the grave over which people are standing in 1945, additional visibility lines were added to the photo (fig. 6).

Figure 6: Additional visibility lines added to photo from 1945.

The geoportal was supplemented with additional visibility lines (fig. 7).

Figure 7: Geoportal was supplemented with additional visibility lines.
An orthophoto from 1945 was used as a base.

The next step was interpretation of a 1944 aerial photo. It was possible to identify a large anomaly visible on the ground. These are probably mass graves. **The line of visibility allowed to determine the place where the people from the photo were gathered.**
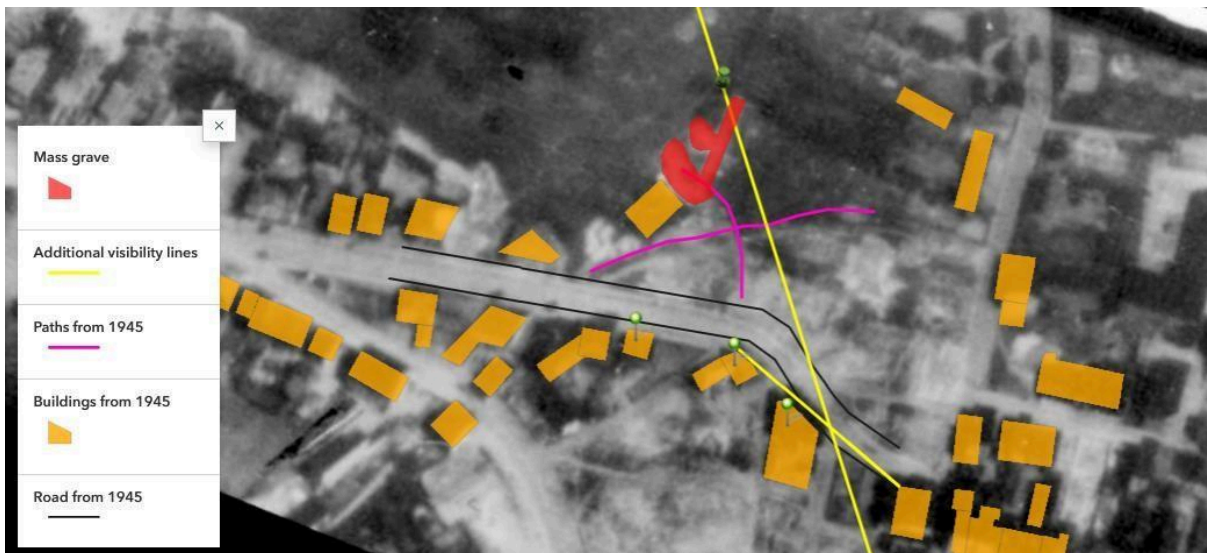

Figure 8. Final Map. The pin marks the place where the photo was taken. An orthophoto from 1944 was used as a base.

Summarising, based on the process described above, it was possible to indicate the most probable location of the mass grave on the cemetery and designate the area for further geophysical research in the field. The area was designated in the field thanks to geodetic measurements and this way the results of the aerial photo interpretation were transmitted into the topography of the Jewish cemetery.


```
Gr_2_1  527108.400  5643412.531
Gr_2_2  527111.192  5643406.979
Gr_2_3  527114.033  5643408.808
Gr_2_4  527111.511  5643412.799
Gr_2_5  527111.230  5643409.861
utm34N
```

In result, detailed coordinates were obtained indicating the area (listed in the image above), allowing for identifying the designated area in the field.

The ground-penetrating radar research and the magnetometer research was carried out in the field within the identified area (research process and results described below).

Interpretation of geophysical research using ground-penetrating radar

Method

Ground-penetrating radar (GPR), also known as georadar, is a high-resolution and mobile geophysical method. GPR uses high-frequency radio waves (usually in the range of 10 MHz to 2.6 GHz). The GPR transmitter and antenna emit an electromagnetic wave into the ground. When it encounters a subsurface object or a boundary between materials with different electrical permittivities, the wave can be reflected, refracted, or scattered back to the surface. The receiving antenna records changes in the return signal. The principles of operation are similar to seismic methods, but GPR methods use electromagnetic waves instead of acoustic waves. The depth of GPR investigation can be limited by the electrical conductivity of the ground, the frequency of the transmitted signal, and the radiated power. Increased electrical conductivity attenuates the introduced electromagnetic wave, reducing the penetration depth. Higher frequencies do not penetrate as deeply as lower frequencies but can provide better resolution. Analysis of such measurement data is possible thanks to specialised software that generates images resembling cross-sections of the surveyed medium. Examples of such cross-sections include geological stratification of soils and rocks, construction structures (e.g., roads, bridges), underground obstacles and voids, archaeological artefacts, underground installations, and many more.

In the discussed case, the surveys were conducted using a Mala RAMAC GPR device with a shielded antenna operating at 500 MHz. Data were collected along 5 parallel profiles on the right side of the sidewalk and 3 parallel profiles on the left side. The profiles were spaced about 1 metre apart, while the width of the separating sidewalk was 3 metres. The length of each profile was approximately 22 metres.

Processing

The data processing was carried out using standard procedures, with slightly varying parameters for each profile. Based on geological data, the average electromagnetic wave velocity in the surveyed formations was estimated at 0.13 m/ns. The following processing sequence was applied:

- *Move Starttime*: This procedure aims to correct the zero signal. It is performed separately for each profile by shifting the zero time to the first wave entry, to correct the depth. For the WYS1 profiles, this correction was -3.2 ns.

- *Bandpass Butterworth* 350-650 MHz: This is a Butterworth bandpass filter designed to cut off signals with frequencies significantly higher or lower than the signal transmitted from the antenna. In this case, a 300 MHz window was used to ensure that the central frequency corresponds to the antenna frequency.

- *Subtract Mean (Dewow)*: This filter calculates the mean value for each profile using a time window provided as a filter parameter. The calculated mean value is subtracted from the central value, allowing the removal of low-frequency drifts, known as "wowing."

- *Subtract DC Shift*: This procedure aims to remove noise generated by the equipment and associated with DC power supply. This procedure is essential when processing data from older types of antennas. The time window was chosen to bypass the high-amplitude part of the signal and focus only on its final segment, from 15 to 60 ns.

- *Background Removal*: This filter removes background noise and other disturbances that are not relevant to the survey. This results in more precise outcomes and allows for a more accurate representation of the subsurface structure.

- *Time Cut*: A cut-off filter was also applied to remove the part of the recording where no useful signal is expected. In this case, the signal below 50 ns was cut.

- *Gain Function*: This function normalises the signal amplitude across the entire data set by applying a gain function to all profiles.

These filters are crucial in GPR signal processing as they enable the effective removal of disturbances and improve the quality of the obtained results.

Results

The figures below show echograms for successive profiles labelled as OSW1_01 - OSW1_08. The profiles to the east of the sidewalk are presented first (Fig.9 - Fig.13.), with the numbering increasing as they move away from it. Next, the results for the profiles to the west of the sidewalk are presented (Fig.14.-Fig.16.), where the numbering also increases with distance from the obstacle. A characteristic feature of all the discussed profiles is the difference in the geoelectric parameters of the medium along each profile. There is a clear increase in wave attenuation in the initial parts of the profiles compared to the final parts.

This boundary can be defined between 10 and 12 metres of the profile. This also affects the maximum penetration depth, which is greater for the final parts of the surveyed profiles. There is also a strong differentiation between the profiles to the east and west of the sidewalk.

Signal amplitude attenuation occurs predominantly in the profiles located to the east of the sidewalk (OSW1_01-OSW1_05) in their initial parts. This effect is strongest for the first three profiles and weakens as the distance from the sidewalk increases. This may be related to the different material lying at relatively shallow depths. Such signal attenuation is associated with an area of reduced resistivity. It could be due to local alluvium or clay in this area, but it is more likely an artificially deposited material.

All profiles show diffraction hyperbolas, which are quite numerous, but they dominate in shallow layers and are very short and local. The marked hyperbolas have significantly larger arms drawn for better readability. The maximum of the hyperbola is essential in the interpretation. Most of them can be attributed to depths not exceeding 1 metre below the surface. This depth is estimated based on the average wave velocity in the medium, so slight deviations in depth are possible. In some cases, hyperbolas also occur at shallower depths. They appear much more frequently in the initial parts of the profiles on the eastern side of the sidewalk. The group occurrence of diffraction hyperbolas in a small area is very characteristic, which may indicate strongly changing physical parameters over a small area. Slight discrepancies between the profiles may result from measurement difficulties. It should be noted that the distance along the profile is determined using an odometer (a wheel attached to the antenna), which has some measurement uncertainty.

For the profiles labelled as OSW1_01 and OSW1_02, there is an accumulation of anomalies between the 4th and 12th metres of the profile, with no significant signal changes in the further parts. The strongest anomalies are visible on the profile labelled as OSW1_03, appearing from the very beginning of the profile. In the case of the other two profiles on the eastern side, anomalies in their initial parts are less pronounced than in the previous profiles, with others appearing in the later parts. In this case, it should be noted that the last two profiles were conducted in the immediate vicinity of trees and shrubs.
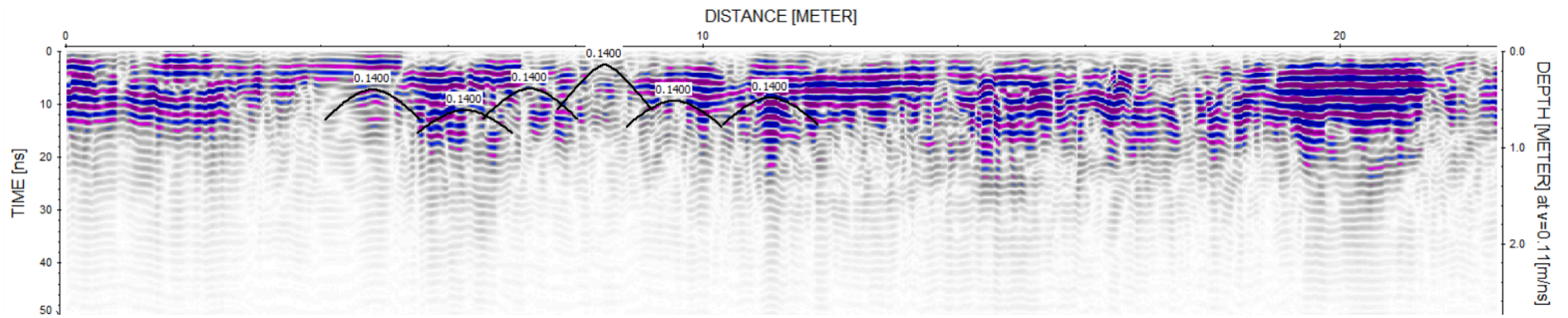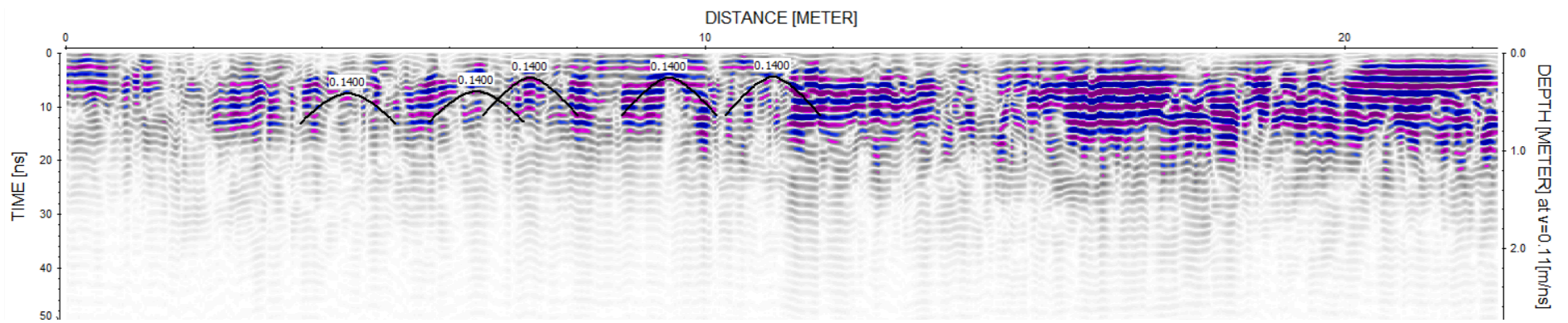
Fig.9. Profile OSW 1_01
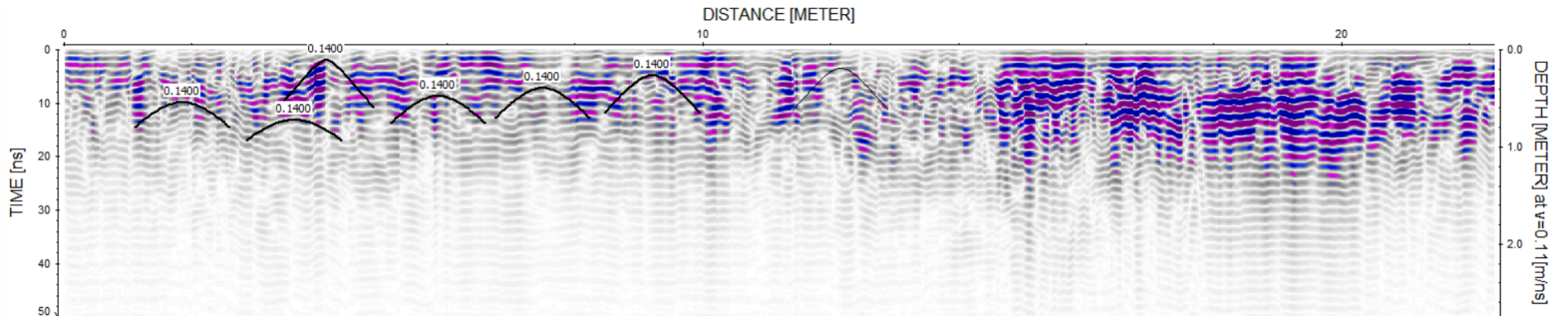

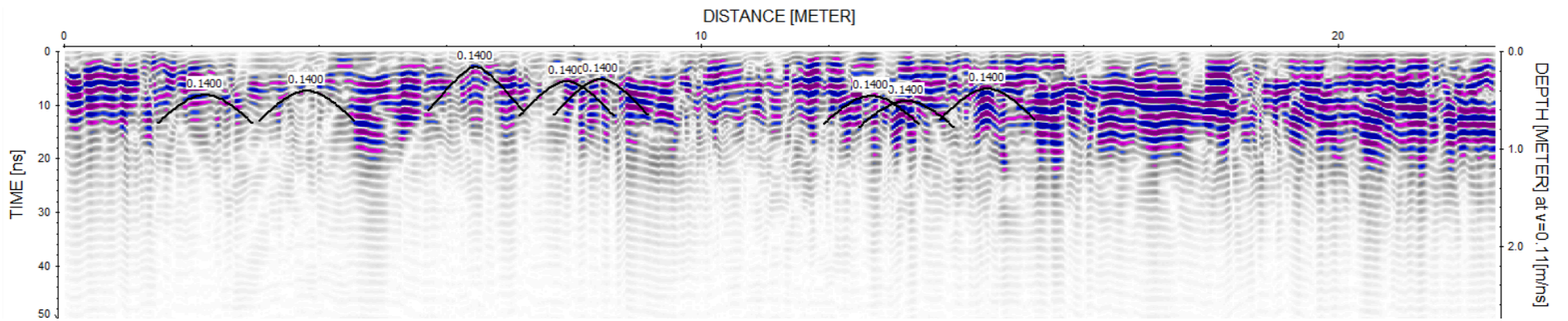*Fig.10. Profile OSW 1_02*

Fig.11. Profile OSW 1_03

Fig.12. Profile OSW1_04

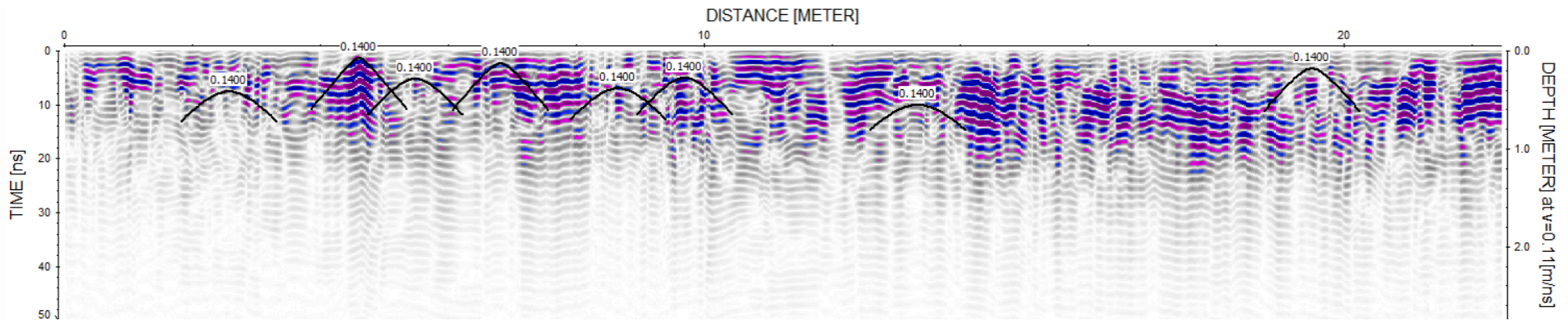*Fig.13. Profile OSW1_05*

In the case of profiles conducted on the other side of the sidewalk (OSW1_06-OSW1_08), there is no such strong differentiation in electromagnetic wave attenuation along the profile length. Only around the 10th to 13th metres in the profiles OSW1_06 and OSW1_07 does a slight effect appear. Regarding the diffraction hyperbolas, they occur in much smaller numbers and do not form distinct clusters, unlike those discussed earlier.
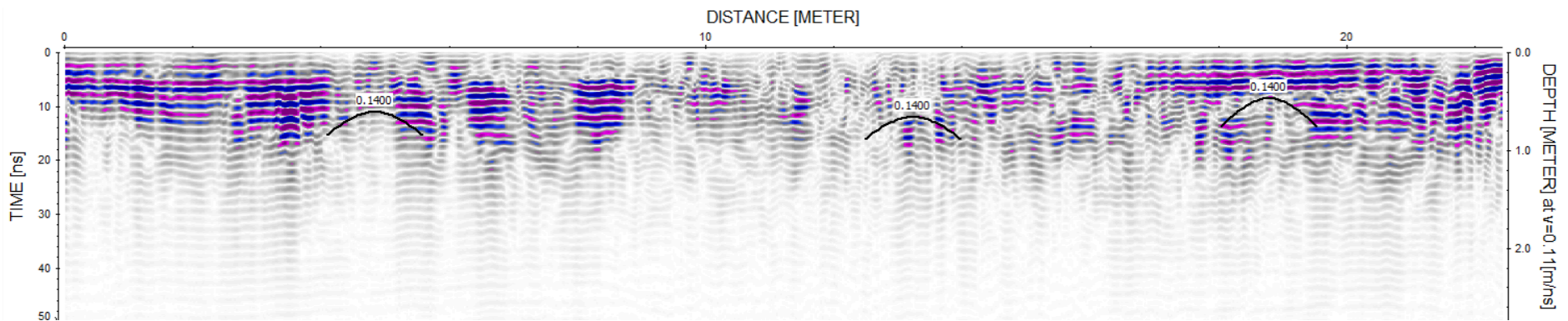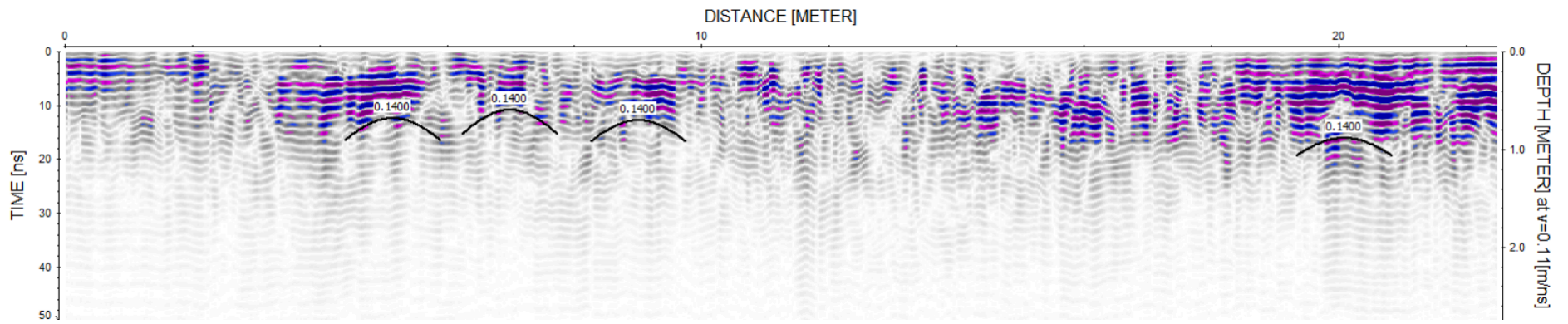

Fig.14. Profile OSW1_06

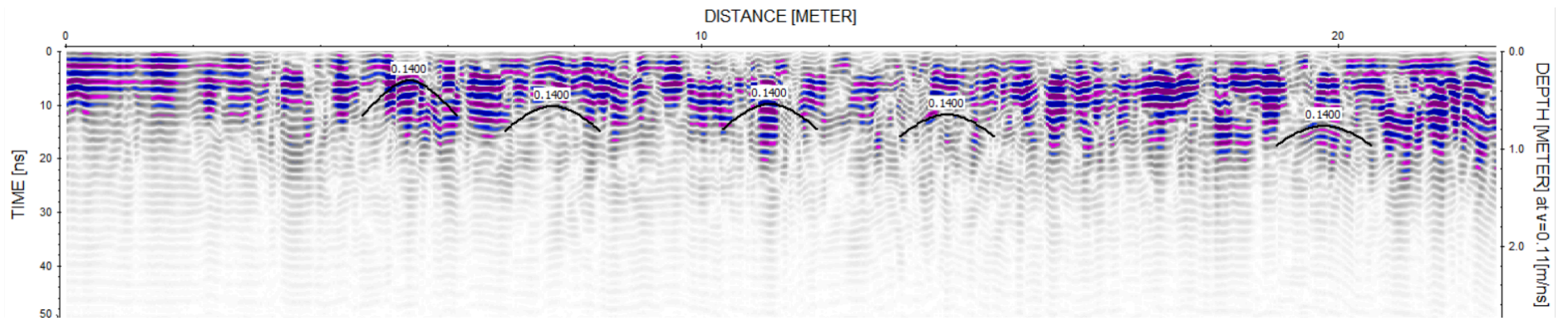*Fig.15. Echogram Profile OSW1_07*

Fig.16. Echogram Profile OSW1_08

In the processed echograms, the hyperbolas dominate in a very shallow range; the hyperbolas visible in the raw data from greater depths are no longer observable. Most likely, these are multiple reflections that were eliminated during processing.

As a summary of the interpretation, a 3D image was created, from which a horizontal cross-section was cut for the depth range of 80 cm to 110 cm below the ground surface. This image is, of course, averaged, but it allows for capturing the approximate location of the strongest anomalies. These are marked in the figure below (Fig.17.) with a red circle. A second area of anomalies is marked with a blue circle, but it is much less distinct and, more importantly, intersected by the sidewalk – making it difficult to determine its origin definitively.
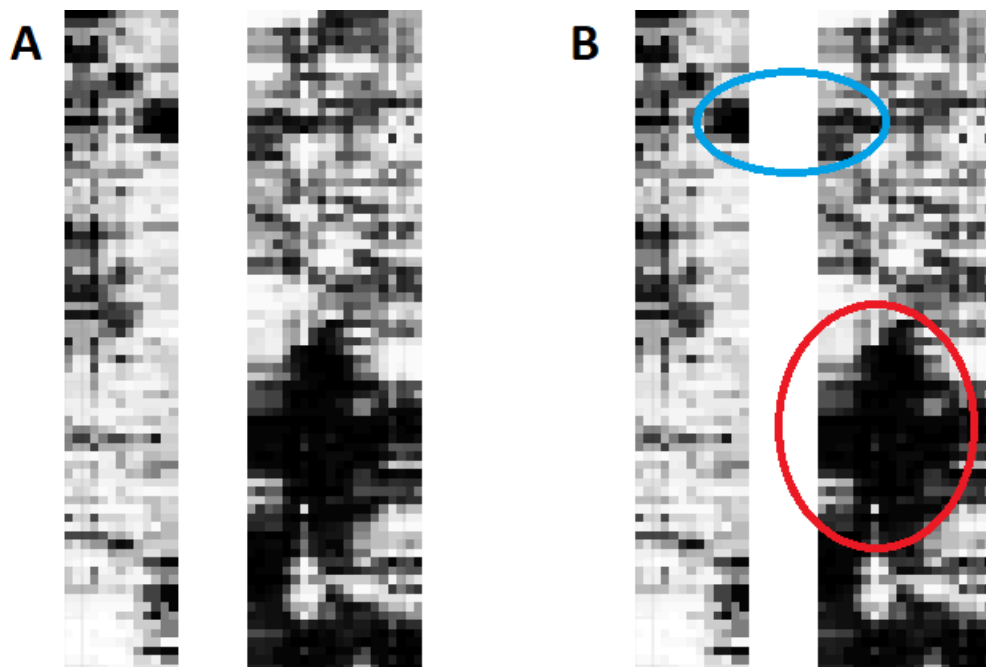

Fig.17. Averaged horizontal cross-section between profiles for depths of 80-110 cm below ground level. A - raw image, B - image with marked anomalies.

The numerous shallow diffraction hyperbolas, corresponding in velocity to the layers in which they are found, may indicate local changes in the dielectric constant of the surveyed medium. Considering the location of the surveys, the clustering of such diffraction hyperbolas can be associated with the presence of burial sites. The shallow depth may be related to the top layer of material that was used to fill the grave, which differs from the surrounding layers and was subsequently covered with a thin (50 cm?) uniform layer as part of land levelling.

Interpretation of geophysical research using a magnetometer

Method

Magnetometry is a non-invasive and surface geophysical method that measures the intensity of the Earth's magnetic field. Changes in this field allow the discovery of various magnetic properties of the medium, which has applications in multiple fields. It is used in geology to identify magmatic structures and in engineering to examine pipelines and detect unexploded ordnance. In archaeology, it allows for the mapping of buried structures and hearths, or graves.

Objects within the range of the magnetic field undergo induction, meaning they become magnetised. The degree of magnetization depends on the intensity vector T and the magnetic susceptibility of the substance, which allows for the classification of bodies into different groups. Diamagnetics, paramagnetics, and antiferromagnetics are bodies with varying levels of magnetization. However, ferromagnetics have the strongest interaction with the magnetic field, causing disturbances in its intensity.

These anomalies are identified in exploratory magnetometry. Through this method, we can infer the presence of various ferromagnetic structures and objects within the Earth's crust. The discovery of such objects can be associated with metal ores, crystalline deposits, magmatic veins, or the location of archaeological artefacts or historical relics. Magnetometry also allows for the detection of underground utility networks.

In this case, a variant of the magnetometric method was used—the measurement of the vertical gradient of the field. This technique involves simultaneously measuring the magnetic field with two sensors spaced apart. The greater the distance between the sensors, the greater the range of this method, allowing for deeper investigations. The main area of application for this method is archaeological research. It is a dedicated tool that enables the effective discovery of buried structures and hearths without the need for simultaneous reference measurements. This simplifies the research process, and the results are accurate and precise.

Processing

The measurement was conducted in a quasi-regular measurement grid, taking into account areas where the measurement was not possible due to dense undergrowth or trees. Data processing was carried out using standard procedures. Measurements that were disturbed, saturated, or had point anomalies (so-called spikes) were not considered for further

processing. Such point anomalies were identified as points with values exceeding 500 nT/m relative to both neighbouring measurement points. The data was then interpolated using the kriging procedure, simultaneously excluding areas not covered by data. In the figures, areas with positive vertical gradient values are marked in red, while those with negative values are marked in green.

Results

The research was conducted on two very closely located survey polygons in the immediate vicinity of the Jewish Cemetery in Ostrowiec Świętokrzyski. These surveys were carried out on two separate research polygons divided by a sidewalk. They will be presented together with the marked structure that separates them. Unfortunately, the survey area poses challenges for this research method. It is situated in close proximity to a metal fence, which borders the study area to the east, and near a metal bench, both of which influence the measurement results. The following figures (Fig.18.-19.) show the results of the spatial distribution of the vertical magnetic gradient.

The magnetic gradient is calculated as the difference between the reading on the lower sensor and the reading on the upper sensor. For these measurements, the distance between the sensors was 1 metre, as we focused on the effects of near-surface structures. A positive magnetic effect should be obtained directly above areas rich in ferromagnetic objects, while a negative effect should be observed at a certain distance from them. Due to the proximity of metal elements, such as the aforementioned fence and bench, the extreme values visible on the map of the vertical magnetic field gradient distribution should be associated with these objects. However, from the perspective of the sought-after object, the most promising area is the section with elevated values in the central part of the area.
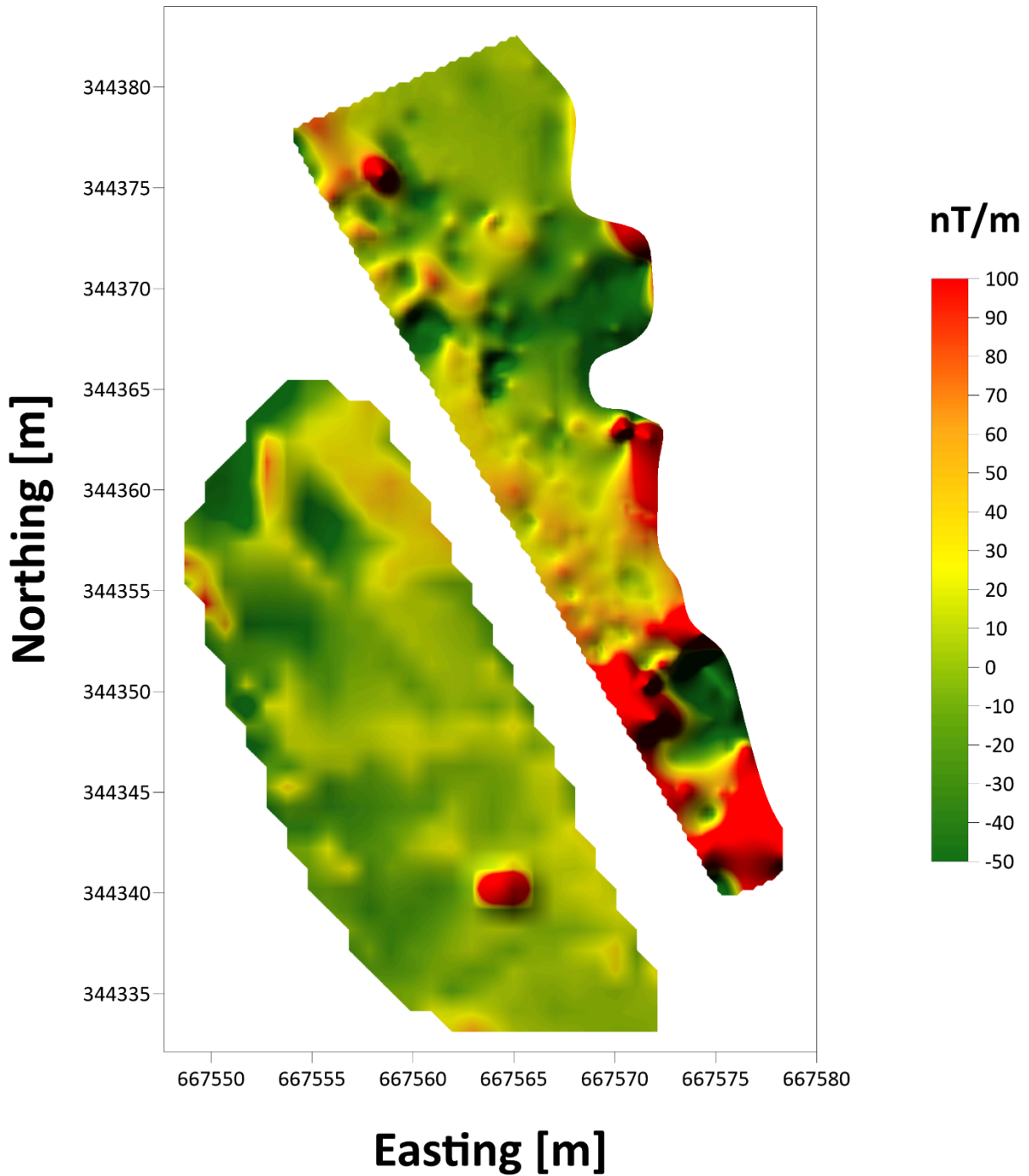
Vertical Magnetic Gradient

Fig.18. Distribution of the vertical magnetic field gradient within the study area in the PL1992 coordinate system.

Magnetic effects originating from graves or buried human remains are orders of magnitude smaller than the effects from metal elements on the surface. Accurately determining the grave area seems impossible due to the aforementioned objects, but the described structure

in the central part of the area, marked on both sides of the sidewalk, provides some prospects, especially when compared with results obtained from other geophysical methods, such as GPR. The figure below (Fig.19.) shows the distribution of anomalies in the vertical magnetic gradient, with the most promising area for the presence of a mass grave marked in blue.
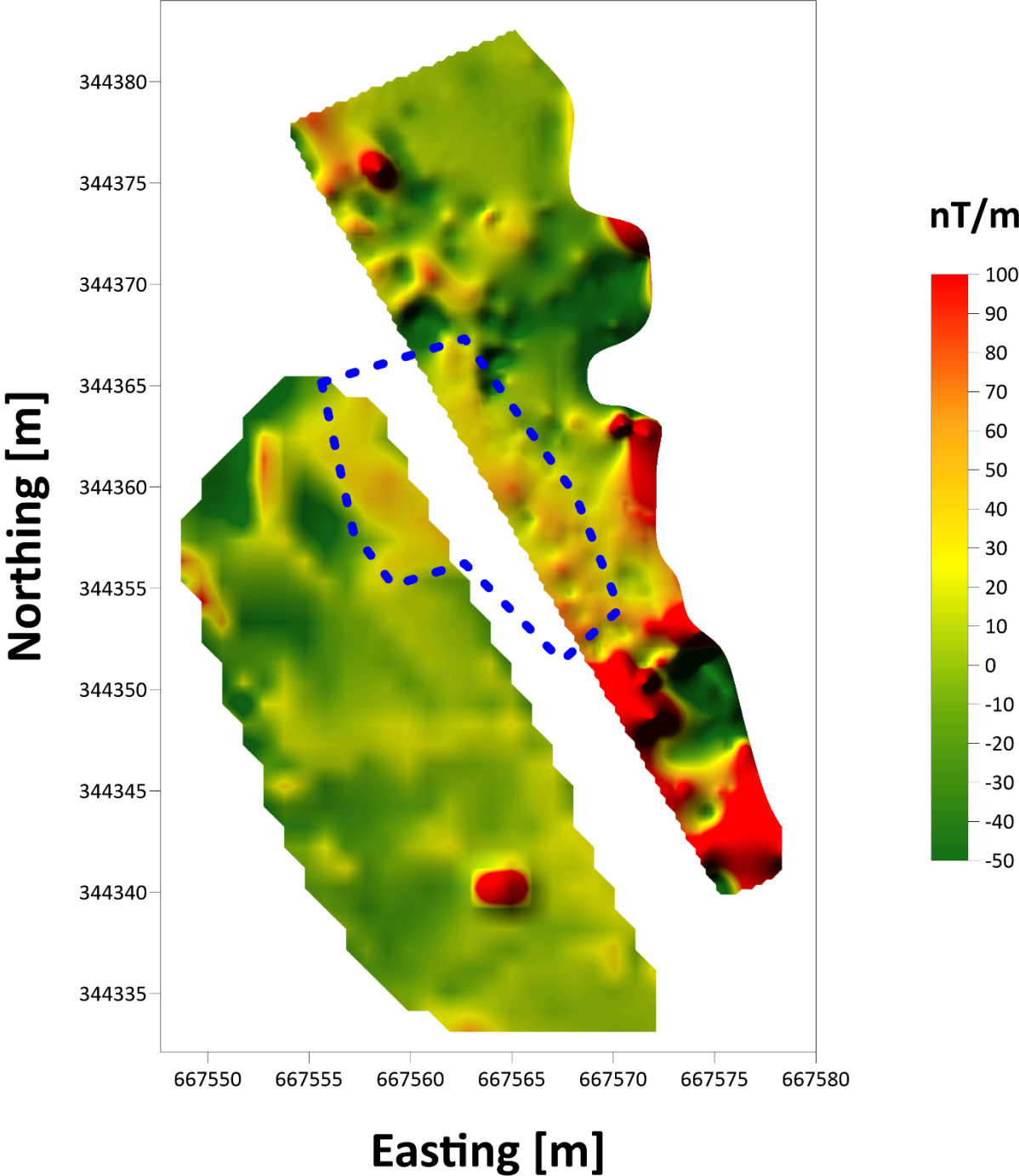
Fig.19. Distribution of the vertical magnetic field gradient in the vicinity of the study area, with the potential mass grave area marked in blue.

In summary, it is very difficult to definitively delineate the boundaries of the sought-after objects in this case. However, it is possible to successfully highlight areas with a positive magnetic effect, which directly correlates with the sought-after objects. This confirms their presence but prevents precise mapping.

Interpretation of conductometric tests

Method

The geoelectric conductivity meter (also named FDEM or slingram) is one of the electromagnetic methods used in geophysics. Central to the operation of a conductivity meter is how current is generated, transmitted and received. The conductometer uses two coils spaced at 's'. The first of these coils, the transmitting coil, is a source of low-frequency current (several to tens of kHz). When the current flows through the transmitting coil, this generates an alternating magnetic field character, denoted as the primary field - Hp. This primary magnetic field is crucial because it penetrates the rock medium. As a result, eddy electric currents are generated in the medium, resulting in secondary magnetic induction. The receiving coil plays an equally important role. It records the secondary magnetic field created in the rock medium. This works on the principle of magnetic induction, which leads to a current flowing in it.

There is a direct correlation between the conductivity of a medium under the influence of magnetic induction and the difference in magnetic field strength between the field generated in the transmitting coil (Hp) and that recorded by the receiving coil (Hs). A conductivity meter with six pairs of transmitting and receiving coils was used during the investigations, allowing the conductivity of the soil to be measured simultaneously at six depths. Two parameters are measured simultaneously during the survey: the apparent conductivity to record changes in the ground conductivity conditions and the relative value of the vertical component of the magnetic field. This so-called in-phase parameter enables the detection of underground metallic objects.

Processing

The survey was carried out in a quasi-regular grid, including areas where this measurement was impossible - dense scrub/trees. Data processing was performed using standard procedures. Disturbed and overdriven measurements, as well as point anomalies (so-called

pins), were not taken into account for further processing. A one-dimensional interpretation of the conductivity data was performed, i.e. a model curve was calculated for each field curve so that the fitting error was as low as possible. A value of no more than 5% was considered an acceptable error. The 1D interpretation was performed separately for each measurement point, which was treated as a sounding. The data were then interpolated using a kriging procedure while excluding areas not covered by the data. The figures show places with low resistivity values in blue, while those with high resistivity values are shown in red.

Results

The research was conducted on two very closely located survey polygons in the immediate vicinity of the Jewish Cemetery in Ostrowiec Świętokrzyski. These surveys were carried out on two separate research polygons divided by a sidewalk. They will be presented together with the marked structure that separates them. Unfortunately, the survey area poses challenges for this research method. It is situated in close proximity to a metal fence, which borders the study area to the east, and near a metal bench, both of which influence the measurement results. The following figure (Fig.20.) shows the spatial distribution results of the electrical resistivity at six different depths below the ground surface, respectively (25cm, 50cm, 80cm, 110cm, 160cm and 230cm).
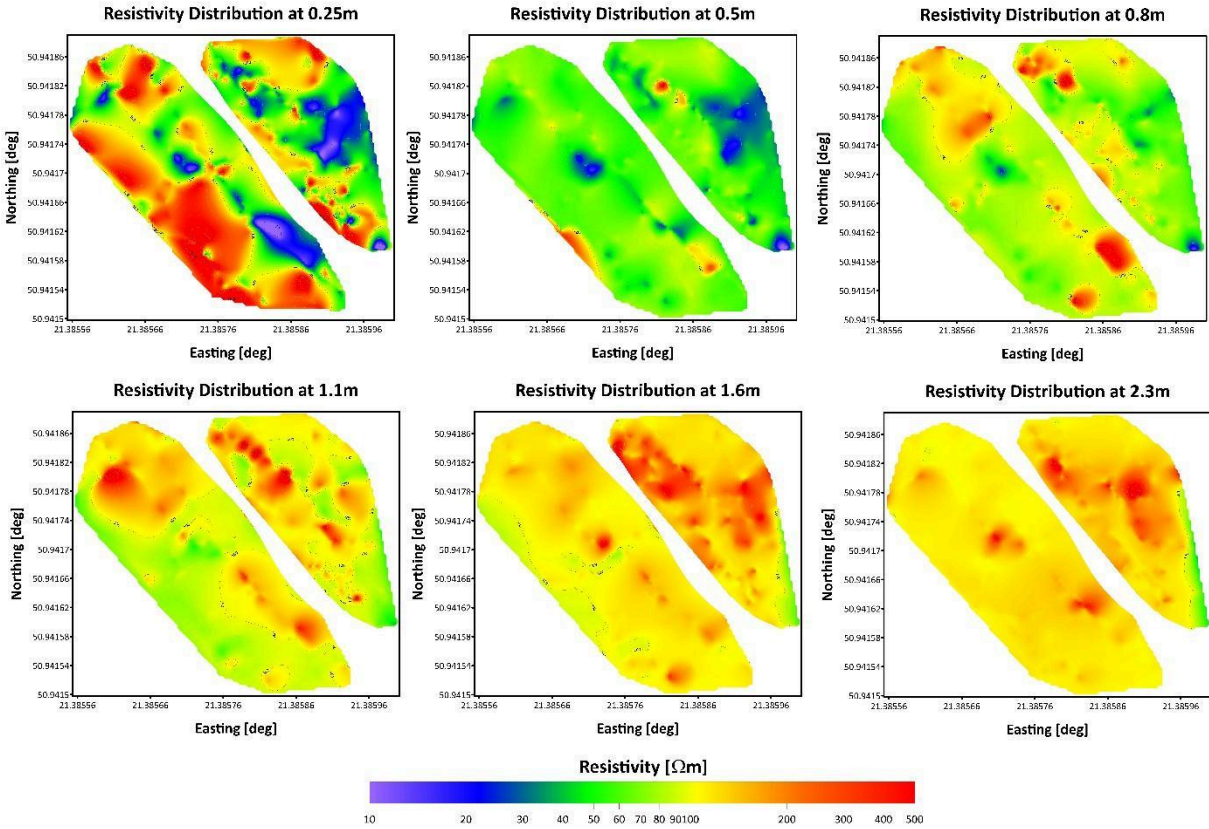

Fig.20. Summary of electrical resistivity distribution at six different depths below the ground surface.

Based on the analysis of resistivity distribution maps obtained using the conductivity method (slingram), it is possible to identify areas characterised by significantly higher electrical resistivity than the surrounding environment. This method allows for investigating subsurface resistivity variations, which is crucial for identifying structures with differing physical properties. However, interpreting the results, especially for the shallowest layers, such as those 25 cm below the surface, poses a challenge. This is because the resistivity in this layer can be influenced by subsurface structures and objects present on the surface, leading to significant variability in the results.

A critical issue in this analysis is the influence of a metal fence located in the eastern part of the study area. Its presence causes a noticeable reduction in resistivity, which can be observed on all maps, regardless of the depth of the measurement. This effect, visible at all analysed depths, is an artefact of the measurement and should not be considered when interpreting the results. The marked drop in resistivity caused by the fence distorts the local resistivity distribution, but excluding this factor allows for a more accurate analysis of the remaining areas.
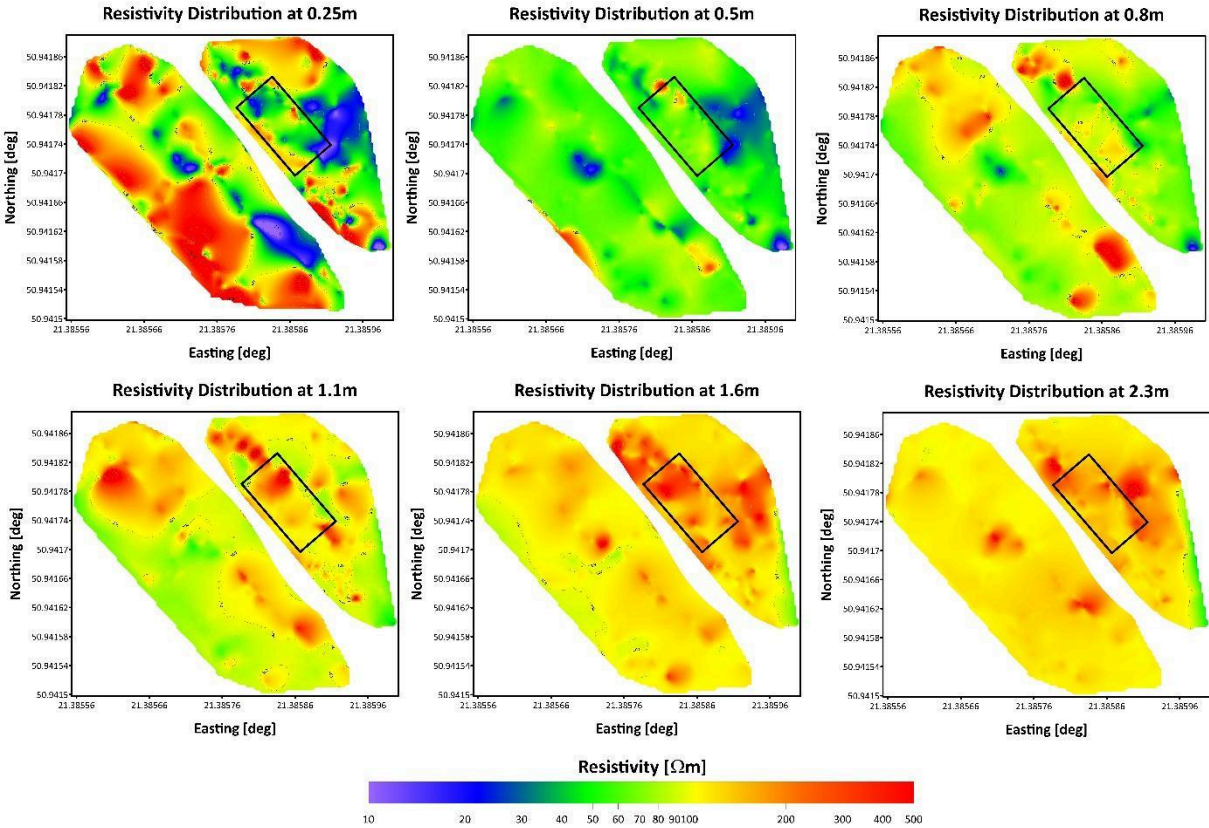

Fig.21. Summary of electrical resistivity distribution at six different depths below the ground surface with the outline marked in a black rectangle.

From the object of interest perspective, special attention should be given to the zone of elevated resistivity located in the central part of the eastern area. On the maps representing depths below 1 meter, this area stands out with significantly higher electrical resistivity, suggesting the presence of an underground structure or geological anomaly with different properties. This zone has been marked with a black rectangle in Figure 21 (Fig.21.), highlighting its significance for further investigation.

Notably, in this area, but at shallower depths, a reduction in resistivity is predominant. This phenomenon may indicate the presence of a previously excavated area that has since been backfilled, potentially altering the local electrical properties of the ground. This interpretation is further supported by the fact that other parts of the study area do not exhibit significant resistivity variations with depth. **Therefore, the concentration of resistivity changes in this specific zone is unique and suggests that it may conceal interesting subsurface structures that warrant further, detailed investigation. This also points to this location's potential significance in searching for objects of historical importance.**

In summary, in this case, it is challenging to delineate the boundaries of the sought-after objects definitively. However, it is possible to successfully highlight areas characterised by a marked change in vertical resistivity. These measurements confirm their presence but prevent precise mapping.

Summary of the research results

After analysing and comparing the research results from the entire research process, the research team consisting of Sebastian Różycki, PhD, Szymon Oryński, PhD and Aleksander Schwarz has indicated the most probable location of the mass grave at the Ostrowiec Świętokrzyski cemetery visible in the data discussed above. Their initial research findings from August 2024 were supported by the results of the conductometric tests carried out in October 2024.